



# Predicting the gravity-driven flow of power law fluids in a syringe: a rheological map for the IDDSI classification

Rémi Lecanu<sup>1</sup> · Guy Della Valle<sup>2</sup> · Cassandre Leverrier<sup>1</sup> · Marco Ramaioli<sup>1</sup>

Received: 20 February 2024 / Revised: 2 April 2024 / Accepted: 3 April 2024 / Published online: 22 May 2024  
© The Author(s), under exclusive licence to Springer-Verlag GmbH Germany, part of Springer Nature 2024

## Abstract

Food rheology is key to manage the swallowing safety of people affected by swallowing disorders (dysphagia). Simple approaches to assess the flow properties of texture-modified drinks are widely used, but relatively poorly understood. This study focuses on the International Dysphagia Diet Standardisation Initiative (IDDSI) flow test, adopted by caregivers worldwide. This test considers the gravity-driven flow in a vertical syringe. Newtonian liquids and non-Newtonian fluids obtained using a commercial starch-based thickener were considered in this study. An accurate theoretical description of the flow is proposed for Newtonian and power-law fluids considering the effect of fluid properties and of the syringe geometry. A rheological map is proposed, based on the results of several thousand simulations, to capture quantitatively the effect of rheological properties and density on the IDDSI classification, highlighting the important effect of the fluid density which is usually ignored. The sensitivity of the IDDSI results with respect to the syringe outlet diameter is discussed, as well as the different average shear rates at which different IDDSI levels are tested. The rheological map also shows quantitatively that different combinations of the fluid rheological properties and density can result in the same IDDSI classification, suggesting interesting directions for future clinical research.

**Keywords** Syringe · Non-Newtonian · Rheological mapping · Swallowing disorders

## Introduction

Gravity-driven flow tests are widely used for quality control purposes, such as the Posthumus funnel for dairy products (Hellings et al. 1986), the Marsh cone in civil engineering (Roussel and Le Roy 2005), or the flow cups in the paint industry. Gravity drives the products either through an orifice or a pipe, depending on the device. Usually, the total efflux time for a given volume to flow out of the apparatus is measured. Such tests are popular thanks to their wide

availability, the small volume of product needed and the short testing time, making them ideal devices with good adaptability to the on-field requirements. Therefore, it is not surprising to see similar devices appearing in many other fields, particularly to assess food texture at the point of consumption and manage swallowing disorders.

Dysphagia or swallowing disorders are a symptom of a wide range of conditions that can affect, in particular, older adults. It can arise because of a lack of muscle strength involved in the swallowing process or poor coordination, leading dysphagic patients to be unable to safely transport food products and beverages from the mouth to the stomach. The consequences can be severe and potentially life-threatening: aspiration of food and drinks into the airways can result in pneumonia and asphyxiation. In addition, dysphagia can significantly impact the quality of life, causing malnutrition and dehydration (Clavé and Shaker 2015).

Texture modification of food and drinks effectively reduces such risks and is widely used for managing dysphagia. Dysphagic patients often experience improved swallowing function when consuming thickened liquids (Steele et al. 2015). However, the rheological behaviour depends on the

✉ Marco Ramaioli  
marco.ramaioli@inrae.fr

Rémi Lecanu  
remi.lecanu@agroparistech.fr

Guy Della Valle  
guy.della-valle@inrae.fr

Cassandre Leverrier  
cassandre.leverrier@agroparistech.fr

<sup>1</sup> University Paris-Saclay, AgroParisTech, INRAE, UMR SayFood, 22 Place de l'Agonomie, 91120 Palaiseau, France

<sup>2</sup> UR BIA, INRAE, La Geraudiere, 44000 Nantes, France

thickener, the thickened continuous phase, and the serving temperature, which often evolves with time. While rheometers or viscometers could accurately quantify the flow properties, they are generally unavailable to caregivers and medical facilities. Therefore, more straightforward, alternative approaches are used at the point of consumption to ensure safe and effective texture modification of food and drinks for dysphagic patients. Among them, gravity-driven flow tests are a logical choice.

The International Dysphagia Diet Standardisation Initiative (IDDSI) has developed a texture classification and the associated tests. This study focuses on the IDDSI syringe flow test, a method to assess the IDDSI texture levels of beverages. The test involves pouring 10 mL of the desired drink into a syringe without its plunger and allowing it to flow under the effect of gravity for 10 s. The volume of fluid remaining in the syringe is associated with one of the IDDSI texture levels for liquids. The levels range from thin liquids, safe only for healthy individuals, IDDSI level 0 with less than 1 mL remaining in the syringe and associated with the colour white in the IDDSI representation, to thicker levels suitable for people suffering from dysphagia of increasing severity, IDDSI levels 1, 2, and 3, with residual volume at 10 s being, respectively, between 1 – 4 mL (grey coloured), 4 – 8 mL (pink coloured), and 8 – 10 mL (yellow coloured). The IDDSI flow test provides a simple way of characterising the texture of liquids for dysphagic patients, which can be used by caregivers and medical facilities.

While it has proven useful in practice, it still needs to be clarified how fluid properties affect the test outcome or if any limitations may arise (Cote et al. 2020). Hanson et al. (2019) investigated the shear rates and stress applied to the fluids in the IDDSI syringe flow test to compare its relevance with *in vivo* physiological values during the swallowing process. Using Computational Fluid Dynamics (CFD), they could accurately describe the flow of an extensive range of rheological behaviour, namely Herschel-Bulkley fluids, exhibiting yield stress and a power-law behaviour. CFD can indeed allow accurate results in complex geometries, but these time-consuming simulations limit the range of parameters that can be considered and in turn provide limited physical insight on the effect of the fluid properties on the test result. Matsuyama et al. (2020) proposed an analytical study for Newtonian liquids, with the objective of quantifying the effect of the syringe geometry on the test outcome. However, few food products are Newtonian, which limits the impact of this study.

Given this context, the objective of this article is to understand the flow of Newtonian and power-law fluids in a vertical syringe under the effect of gravity and propose a simple analytical model to study the sensitivity of the IDDSI flow test with respect to product properties and geometrical features. Experimental and modelling results were compared quantitatively, and a map is proposed to capture the effect of the

rheological parameters on the IDDSI levels predicted by the syringe test.

## Materials and methods

This study considers three different groups of fluids, namely (i) Newtonian fluids, (ii) shear-thinning fluids commonly used in the management of dysphagia, and (iii) mixes of the above two, to cover intermediate rheological behaviours.

### Fluid preparation

#### Newtonian solutions

Glycerol aqueous solutions (G) were chosen as Newtonian fluids. The glycerol (GLYCEROL > 99% FCC FG W252506, Sigma-Aldrich, Saint-Louis, Missouri, USA) was mixed with deionised water at different ratios (w/w), chosen to cover the IDDSI levels in the syringe. Each (G) solution was prepared by weighing a mass of distilled water and of glycerol using a  $\pm 0.01$  g balance Sartorius 1475 MP8-2, (Göttingen, Germany) and mixing them in a 200 mL glass beaker with a magnetic mixer at 500 rpm for 5 min, except for the highest concentration for which a rotational speed of 1000 rpm was used. The latter was adapted to obtain a good mix without adding air bubbles in the solutions at  $T = 20^\circ\text{C}$ . For the highest ratio of glycerol, the two liquids were manually mixed beforehand to improve the magnetic stirrer mixing. When the amount of glycerol increases, the solutions' density increases, which must be considered. The density of each sample was measured three times while performing the IDDSI syringe flow test. The difference of mass between the full 10 mL syringe and the empty syringe was recorded to obtain the density value.

A highly viscous Newtonian fluid, General Purpose Viscosity Standard (N), N4000 (VWR International S.A.S, Rosny-sous-Bois, France), was also used to reach a high viscosity value and obtaining a fluid that is not of level 3, which cannot be reached with glycerol-water solutions.

#### Non-Newtonian solutions

A commercially available starch-based thickener (TU) at different concentrations was used (Resource Thicken-UP, Nestlé Health Science, Epalinges, Switzerland). The solutions were prepared by weighing the mass of TU powder using a  $\pm 0.001$  g precision balance Mettler-Toledo AE420 (Greifensee, Switzerland), mixed with 100 g of mineral water (Vittel, Nestlé Waters, Issy-les-Moulineaux, France) in a glass beaker, stirred for 30 s with a metal spatula. They were then left to rest for at least 1 h. Before each use, they were again vigorously stirred in a rotational motion with a

metal spatula for 5 s. The temperature was always maintained at  $T = 20^\circ\text{C}$ . Adding TU to water does not significantly change the density of the liquid. The TU solutions density was measured the same way as for the (G) solutions and showed minimal variation. A standard value of  $1000 \text{ kg} \cdot \text{m}^{-3}$  is chosen for each TU solution in the model described later.

Ternary mixtures of the TU thickener with glycerol and water (GTU) were also prepared to address a broader range of rheological properties. As mentioned, TU is a starch-based thickener that needs water to hydrate and be fully functional. When a high amount of TU is dispersed in concentrated glycerol solutions, the available water becomes limited and does not fully swell the starch granules in the TU powder. So, the ternary solutions were prepared according to two methods, either by (i) thickening aqueous solutions at 67% and 87% part of glycerol, with selected ratios of TU, or (ii) by diluting a highly thickened water, containing 7.41% (w/w) of TU with different ratios of pure glycerol.

For all starch-based solutions (TU and GTU), the IDDSI flow test experiments and the rheological measurements were performed on the same day. For the Newtonian solutions, both tests were done within a 3-day interval.

## Rheological characterisation

To characterise the rheological behaviour of the fluids and extract the parameters needed for the mathematical model, a MCR 702e MultiDrive (Anton Paar GmbH, Graz, Austria) was used in rate-controlled mode with a coaxial cylinder geometry (CC27) and a gap of 1 mm. For all fluids, shear rates ranging from 5 to  $500 \text{ s}^{-1}$  were considered, and this range was further widened for selected fluids, when this did not generate artefacts.

## Surface tension characterisation

The surface tension was measured for the lowest concentration of each G and TU with a plate tensiometer (Processor Tensiometer K12 Mk6, Krüss GmbH Germany), with a plate velocity of 2 mm/min and a depth length of 2 mm. With increasing concentrations of Resource ThickenUp or glycerol, the effect of surface tension on the flow decreases, because of the higher fluid viscosity. Surface tension for fluids above level 2 were not measured and assumed to be equal to the surface tension measured for lower concentrations (level 1), accepting a small overestimation of surface tension that has little impact on the predicted flow.

## Instrumented IDDSI syringe flow test

The IDDSI syringe flow test should be run with a syringe with a distance  $h_0 = 61.5 \text{ mm}$ , between the 0 and 10 mL ticks. In this study, the BD 10 mL syringe with a luer-lock tip (reference: 300912, Becton Dickinson, Franklin Lakes, New Jersey, USA) was used, which is available in Europe and part of the list of Becton Dickinson (BD) syringes recommended by IDDSI (IDDSI 2018). For this syringe  $h_0 = 60.7 \text{ mm}$ . Because many dimensions were of interest for the development of the model, Table 1 encloses the relevant dimensions, and a diagram of the syringe is provided in Fig. 1a.

In this study, 15 syringes of the same reference were used and washed after each use according to the IDDSI recommendations. Given the strong influence of the nozzle outlet radius  $R_{min}$  on the flow (Matsuyama et al. 2020) along the other dimensions,  $R_{min}$  was measured for each syringe, and its variability is reported in Table 1.

A Basler black and white camera acA2440 - 75um (Ahrensburg, Germany), used at 2448x2048 pixel resolution and 25 frames per second, recorded the flow in the syringe with an Opto-Engineering 16 mm Lens model EN5MP1616 (Mantova, Italy). The video was triggered before the start of the IDDSI test. The image corresponding to the end of the 10 s duration of the test was identified after 250 frames, corresponding to 10 s of flow. A led panel was used to back-lit the syringe, thus providing enough contrast for the meniscus to be detected and its position to be identified in each frame via image analysis (Fig. 1b), using the ImageJ software (Schindelin et al. 2012) (Rasband, W.S., ImageJ, U. S. National Institutes of Health, Bethesda, Maryland, USA, <https://imagej.nih.gov/ij/>, 1997-2018.). Each test was run in triplicates. For each repetition, a new volume of 10 mL was poured into the syringe, paying attention to avoid bubbles. All experiments were performed at  $T = 20^\circ\text{C}$ .

According to the IDDSI framework for level 3 fluids, the syringe measurements should be completed with the IDDSI fork drip test, which assesses whether the fluids flow through the prongs of a fork or hold their shape. If it flows, the fluid is a level 3; otherwise, the fluid cannot be described as a level 3 nor a level 4.

## Theory

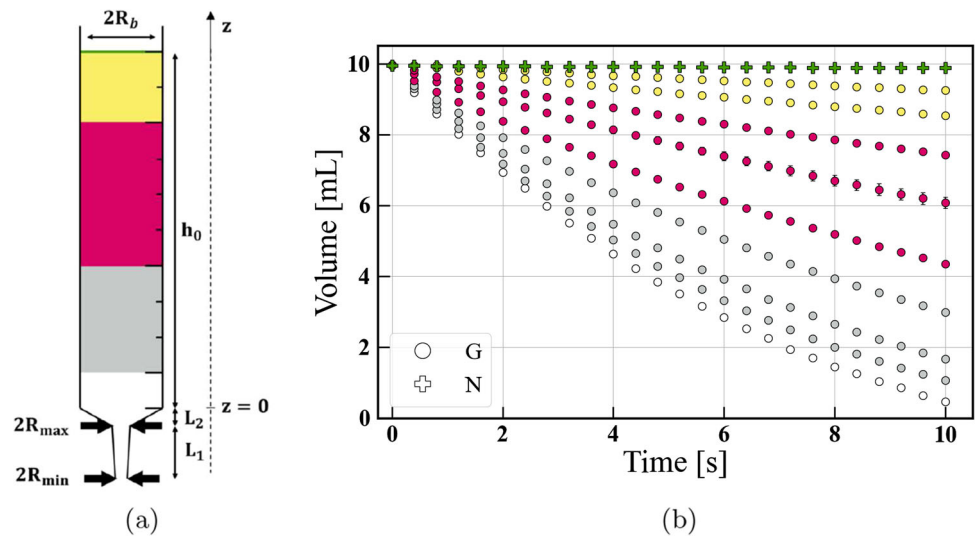
### Assumptions

The theory presented in this paragraph describes the gravity-driven flow of an incompressible fluid in the syringe. The

**Table 1** Main syringe dimensions

| $R_{min}$ [mm]  | $R_{max}$ [mm]  | $R_b$ [mm]      | $L_1$ [mm]      | $L_2$ [mm]      | $h_0$ [mm]       |
|-----------------|-----------------|-----------------|-----------------|-----------------|------------------|
| $0.97 \pm 0.03$ | $1.55 \pm 0.08$ | $7.20 \pm 0.01$ | $9.30 \pm 0.10$ | $3.70 \pm 0.10$ | $60.70 \pm 0.13$ |

**Fig. 1** **a** Schematic representation of the syringe used in the IDDSI flow test and its key dimensions. The initial height of the fluid in the barrel is denoted  $h_0$  and the barrel inner diameter  $2R_b$ . Below the barrel, a cone of length  $L_2$  reduces the inner diameter to  $2R_{max}$ . Finally, a conical nozzle of length  $L_1$  leads to the outlet (diameter  $2R_{min}$ ). **b** Typical evolution with time of the volume of Newtonian liquids in the syringe, measured experimentally. Colours indicate the IDDSI levels obtained from the residual volume at the end of the test



main barrel acts as a reservoir, providing a hydrostatic pressure head to the convergent section. Over time, the lowering liquid height in the barrel leads to a reduction of pressure at the entrance of the convergent section and to a reduction of flow rate. The flow is assumed to be quasi-stationary.

The fluids considered in this study do not exhibit significant elasticity (Mackley et al. 2013). Due to the wider diameter, the viscous dissipation in the barrel is neglected, and only the dissipation in the convergent section and in the nozzle are considered. Inertial effects and dissipation due to sharp corners are also neglected.

Experimentally, it was observed that the more viscous fluids showed a dripping regime throughout the syringe test. In contrast, less viscous ones initially exhibit a jet flow regime and then switch to a dripping regime.

The importance of capillarity can be assessed by considering the Capillary number (Digilov 2008), namely the ratio between viscous and surface tension forces:

$$Ca = \frac{K v_{min}^n}{\sigma} \left( \frac{3n + 1}{R_{min} n} \right)^{n-1} \tag{1}$$

where  $K$  is the consistency index,  $n$  is the flow index, and  $v_{min}$  is the mean velocity in the nozzle at the outlet radius  $R_{min}$ . The maximum value of the Capillary number is 0.32, confirming that the surface tension effect is not negligible and that the Laplace pressure term should be considered in the theory.

The Reynolds number for power-law fluids is defined as (King 2002):

$$Re = \frac{2\rho v_{min} R_{min}}{K} \left( \frac{4n}{3n + 1} \right)^n \left( \frac{8v_{min}}{R_{min}} \right)^{1-n} \tag{2}$$

For all fluids considered, the Reynolds number is below 360, low enough for the system to be considered laminar ( $Re < 2400$ ), which confirms the assumption made in the theory. An increase in viscosity leads to a decrease in the Reynolds number.  $Re$  is lower than  $10^{-3}$  for the most viscous fluids.

The formation of droplets at the exit of the nozzle induces a curvature of the liquid’s free surface. The surface tension is resisting the flow through a constant Laplace pressure that can be written as

$$\Delta P_L = 2 \frac{\sigma}{R_{min}} \tag{3}$$

where  $\sigma$  is the surface tension.

As a result, the pressure head driving the flow in the convergent section can be written as the difference between the hydrostatic pressure  $\Delta P_H$  applied by the liquid in the barrel and the Laplace pressure  $\Delta P_L$ :

$$\Delta P = \Delta P_H - \Delta P_L = \rho g (h_s(t) + L) - 2 \frac{\sigma}{R_{min}} \tag{4}$$

where  $\rho$  is the fluid density,  $g$  is the gravitational acceleration,  $h_s(t)$  is the fluid height in the main barrel, and the total length of the convergent section is  $L = L_1 + L_2$ .

### Hagen-Poiseuille flow in the convergent section

Using the Eulerian form of the Cauchy momentum equation and considering only the gravitational forces as volume forces, the starting equation is

$$\rho \left( \frac{\delta \vec{v}}{\delta t} + (\vec{v} \cdot \vec{\nabla}) \vec{v} \right) = -\vec{\nabla} p + \rho \vec{g} + \vec{\nabla} \cdot \bar{\tau} \tag{5}$$

where  $\vec{v}$  is the velocity vector,  $\vec{\nabla} p$  is the pressure gradient, and  $\vec{\tau}$  is the stress tensor. The nozzle can in first approximation be considered a vertical, cylindrical pipe (along the  $z$  – axis, see Fig. 1a). The nozzle radius is  $r$ , and the no-slip boundary condition is assumed at the lateral wall.

The Eq. (5) is reduced to

$$\vec{\nabla} \cdot \vec{\tau} = \vec{\nabla} p \tag{6}$$

For Newtonian fluids,  $\tau = \eta \dot{\gamma}$ , with  $\tau$  the shear stress,  $\eta$  the viscosity, and  $\dot{\gamma}$  the shear rate, the Hagen-Poiseuille equation is retrieved (Sutera and Skalak 1993):

$$Q = \frac{\pi r^4}{8\eta} \frac{\delta p}{\delta z} \tag{7}$$

A more accurate expression can be derived by considering the effect of the conical nozzle geometry. The entrance and exit radius are labelled  $R_{max}$  and  $R_{min}$ . The varying radius is  $r(z) = a + bz$ , where  $a = R_{max}$  and  $b = \frac{R_{min} - R_{max}}{L}$  (Fig. 1a).

Neglecting the radial velocities and integrating Eq. 7, the Hagen-Poiseuille equivalent for the flow in a cone-shaped pipe gives

$$Q = \frac{\pi \Delta p}{8\eta} \left( \frac{3ba^3(a + bL)^3}{(a + bL)^3 - a^3} \right) \tag{8}$$

### Viscous dissipation of power-law fluids in the convergent section

Power-law fluids can be described by the relation

$$\tau = K \dot{\gamma}^n \tag{9}$$

The dissipation in a conical pipe can be expressed as

$$Q = \frac{\pi n}{(3n + 1)} \left( \frac{\Delta P}{2KA} \right)^{\frac{1}{n}} \tag{10}$$

where  $A = \frac{(a+bL)^{3n} - a^{3n}}{3nba^{3n}(a+bL)^{3n}}$  is a shape factor calculated from the geometrical parameter  $a$  and  $b$  introduced in the previous paragraph.

Both the conical sections at the bottom of the syringe were considered, with  $A_1 = \frac{(a_1+b_1L)^{3n} - a_1^{3n}}{3nb_1a_1^{3n}(a_1+b_1L)^{3n}}$  and  $A_2 = \frac{(a_2+b_2L)^{3n} - a_2^{3n}}{3nb_2a_2^{3n}(a_2+b_2L)^{3n}}$ .

$$Q = \frac{\pi n}{3n + 1} \left( \frac{\Delta P}{2K(A_1 + A_2)} \right)^{\frac{1}{n}} \tag{11}$$

### Considering fluid acceleration when entering the convergent section

When the fluid leaves the syringe barrel, it accelerates to enter the convergent section, thereby increasing kinetic energy at the expense of pressure head. Based on Bernoulli’s principle (Hellinga et al. 1986), the pressure decrease caused by the acceleration throughout convergent section and the nozzle can be written as

$$\Delta P_c = \frac{1}{2} \rho \left( \frac{Q}{\pi R_{min}^2} \right)^2 \tag{12}$$

By combining Eqs. 11 and 12 to write the total pressure loss  $\Delta P$ , a non-linear equation governing the flow in the nozzle is obtained:

$$2K(A_1 + A_2) \left( \frac{1 + 3n}{n\pi} Q \right)^n + \frac{1}{2} \rho \left( \frac{Q}{\pi R_{min}^2} \right)^2 = \Delta P \tag{13}$$

The flow rate exiting the syringe  $Q$  is obtained by finding the root of this equation at each time step. Due to continuity, the flow rate is conserved between the main barrel and the nozzle exit,  $Q = \pi R_b^2 v_s = \pi R_{min}^2 v_{min}$ , and the variation with time of the fluid height  $h_s$  in the main barrel can be obtained:

$$\frac{dh_s}{dt} = - \frac{Q}{\pi R_b^2} \tag{14}$$

The simultaneous solution of the Eqs. 4, 13, and 14 allows computing the evolution with time of the flow rate and of the volume in the syringe.

## Results and discussions

### Rheological properties

The glycerol solutions are Newtonian. Increasing the glycerol concentration increases the viscosity from 0.02 to 1.31 Pa.s (Table 2). The suspensions of TU in water exhibit a shear-thinning behaviour (Fig. 2a) except for the most dilute, TU1, which shows a Newtonian behaviour. Increasing the concentration increases viscosity, while decreasing the slope of the curve, showing that the fluids become more shear-thinning. For the most concentrated solutions, a yield stress is observed.

During the test, the shear stress at the nozzle wall can be evaluated as  $\tau_w = \frac{\Delta P R_{min}}{2L}$ . For a fluid with a density of 1000 kg/m<sup>3</sup> and a surface tension of 72 mN/m, considering 10 mL in the syringe, the shear stress is initially  $\tau_{10} = 22$  Pa, and this is the maximum stress experienced by the liquids in

**Table 2** Properties of the fluids, columns: composition, IDDSI level, density, rheological parameters ( $K$  and  $n$ ), surface tension. Rows: glycerol/water solutions (G), viscosity standard N4000 (N), Thicken-Up in water (TU), and ternary systems glycerol/water/TU (GTU)

|            | Code sample | Glycerol [% w/w] | Thicken-Up [% w/w] | IDDSI Level | $\rho$ [ $kg.m^{-3}$ ] | $K$ [ $Pa.s^n$ ] | $n$               | $\sigma$ [ $mN.m^{-1}$ ] |
|------------|-------------|------------------|--------------------|-------------|------------------------|------------------|-------------------|--------------------------|
| <b>G</b>   | G1          | 67.0             | –                  | 0           | 1160 ± 4               | 0.020 ± 0.001    | 1.00 <sup>b</sup> | 67.6 ± 0.1               |
|            | G2          | 71.0             | –                  | 1           | 1169 ± 7               | 0.027 ± 0.001    | 1.00 <sup>b</sup> | 67.1 ± 0.2               |
|            | G3          | 75.0             | –                  | 1           | 1191 ± 1               | 0.037 ± 0.001    | 1.00 <sup>b</sup> | 66.7 ± 0.4               |
|            | G4          | 79.0             | –                  | 1           | 1188 ± 3               | 0.055 ± 0.001    | 1.00 <sup>b</sup> | 67.4 ± 0.3               |
|            | G5          | 83.0             | –                  | 2           | 1210 ± 3               | 0.089 ± 0.001    | 1.00 <sup>b</sup> | 67.4 ± 0.3 <sup>a</sup>  |
|            | G6          | 87.0             | –                  | 2           | 1215 ± 4               | 0.156 ± 0.002    | 1.00 <sup>b</sup> | 67.4 ± 0.3 <sup>a</sup>  |
|            | G7          | 91.0             | –                  | 2           | 1226 ± 1               | 0.287 ± 0.003    | 1.00 <sup>b</sup> | 67.4 ± 0.3 <sup>a</sup>  |
|            | G8          | 95.0             | –                  | 3           | 1243 ± 2               | 0.588 ± 0.004    | 1.00 <sup>b</sup> | 67.4 ± 0.3 <sup>a</sup>  |
|            | G9          | 99.0             | –                  | 3           | 1250 ± 2               | 1.293 ± 0.025    | 1.00 <sup>b</sup> | 67.4 ± 0.3 <sup>a</sup>  |
| <b>N</b>   | N1          | –                | –                  | 4           | 886                    | 14.026 ± 0.658   | 1.00 <sup>b</sup> | 67.4 ± 0.3 <sup>a</sup>  |
| <b>TU</b>  | TU1         | –                | 2.20               | 0           | 1005 ± 8               | 0.005 ± 0.001    | 1.00 <sup>b</sup> | 63.7 ± 1.6               |
|            | TU2         | –                | 3.27               | 0           | 1002 ± 4               | 0.040 ± 0.001    | 0.82 ± 0.003      | 57.8 ± 1.9               |
|            | TU3         | –                | 4.03               | 1           | 1006 ± 10              | 0.477 ± 0.039    | 0.58 ± 0.02       | 57.8 ± 1.9 <sup>a</sup>  |
|            | TU4         | –                | 4.31               | 2           | 1011 ± 10              | 0.978 ± 0.118    | 0.53 ± 0.02       | 57.8 ± 1.9 <sup>a</sup>  |
|            | TU5         | –                | 4.76               | 2           | 1009 ± 1               | 1.871 ± 0.324    | 0.49 ± 0.02       | 57.8 ± 1.9 <sup>a</sup>  |
|            | TU6         | –                | 5.04               | 3           | 1010 ± 4               | 5.582 ± 0.909    | 0.38 ± 0.03       | 57.8 ± 1.9 <sup>a</sup>  |
|            | TU7         | –                | 6.32               | 4           | 1012 ± 5               | 17.539 ± 2.985   | 0.36 ± 0.04       | 57.8 ± 1.9 <sup>a</sup>  |
|            | TU8         | –                | 7.41               | 4           | 1008 ± 4               | 45.642 ± 2.396   | 0.35 ± 0.01       | 57.8 ± 1.9 <sup>a</sup>  |
| <b>GTU</b> | G1TU1       | 65.5             | 2.20               | 2           | 1169 ± 3               | 0.191 ± 0.036    | 0.84 ± 0.03       | 72.0 <sup>a</sup>        |
|            | G1TU2       | 64.8             | 3.27               | 3           | 1169 ± 9               | 2.239 ± 0.051    | 0.60 ± 0.01       | 72.0 <sup>a</sup>        |
|            | G1TU3       | 64.3             | 4.03               | 3           | 1167 ± 4               | 4.397 ± 0.210    | 0.57 ± 0.01       | 72.0 <sup>a</sup>        |
|            | G1TU4       | 64.1             | 4.31               | 3           | 1170 ± 8               | 5.712 ± 0.224    | 0.54 ± 0.01       | 72.0 <sup>a</sup>        |
|            | G1TU5       | 63.6             | 5.03               | 4           | 1161 ± 7               | 15.928 ± 1.883   | 0.47 ± 0.02       | 72.0 <sup>a</sup>        |
|            | G6TU1       | 85.0             | 2.20               | 3           | 1226 ± 10              | 0.861 ± 0.063    | 0.86 ± 0.01       | 72.0 <sup>a</sup>        |
|            | G6TU2       | 84.2             | 3.27               | 3           | 1234 ± 29              | 5.384 ± 0.255    | 0.71 ± 0.01       | 72.0 <sup>a</sup>        |
|            | G6TU3       | 83.4             | 4.03               | 3           | 1217 ± 1               | 9.076 ± 0.400    | 0.67 ± 0.01       | 72.0 <sup>a</sup>        |
|            | TU8G1       | 30.0             | 5.19               | 3           | 1098 ± 8               | 10.575 ± 2.062   | 0.40 ± 0.01       | 72.0 <sup>a</sup>        |
|            | TU8G2       | 20.0             | 5.93               | 4           | 1054 ± 2               | 19.473 ± 0.283   | 0.40 ± 0.01       | 72.0 <sup>a</sup>        |

<sup>a</sup>The surface tension of these fluids has not been measured and is only estimated (see “[Surface tension characterisation](#)”)

<sup>b</sup>For these fluids, it is assumed that  $n = 1$

the syringe flow test. As shown by the vertical black lines in Fig. 2a and b, in the range of stresses between  $\tau_1$  and  $\tau_{10}$ , the viscosity can be described well by the power-law model during the flow in the syringe, with no need to consider more complex models, such as the Herschel-Bulkley model. Furthermore, additional measurements were performed on the three highest concentrations of TU, namely TU6, TU7, and TU8 to reach lower shear rates and extract more accurately a yield stress from the flow curves. TU8 shows the highest yield stress  $\tau_{0,TU8} = 5.2 Pa$ , but this is significantly lower than  $\tau_{10}$ . This confirms that all fluids are flowing and the power-law model can be applied.

All ternary mixtures of water, glycerol, and Thicken-Up show shear-thinning behaviour (Fig. 2b) with higher values of

$n$  than for the binary TU water systems and similar  $K$  values (Table 2). The G6TU solutions (Fig. 2b, black triangles) are less shear-thinning than the G1TU (Fig. 2b, white triangles) solutions and the TU7G (Fig. 2b, grey triangles). The last two have an equivalent range of  $K$  and  $n$ .

## Experimental results and comparison with the theory

Pure glycerol is classified as IDDSI level 3 and glycerol-water solutions from level 0 to level 3. Some TU, GTU, and N solutions show almost no flow with only one or two droplets during the total testing time of 10 s, they cannot be identified as level 3. Following the IDDSI (2002) approach,

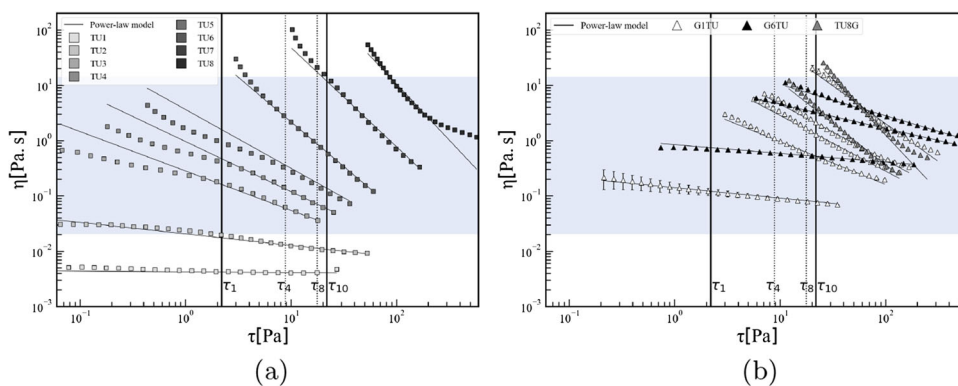


**Fig. 2** Viscosity curves of **a** the aqueous suspensions of TU (compositions indicated in Table 2) and **b** the suspensions of TU in glycerol/water solutions; the three GTU formulations are identified by the colour of the marker: white (thickened G1), grey (thickened G6), and black (diluted TU8), see Table 2. The blue-shaded background shows the range of viscosity of the Newtonian liquids considered in the study. The vertical solid black lines represent the shear stresses in the nozzle experienced

by the fluids throughout the test. The highest stress is labelled  $\tau_{10}$  and is caused by the hydrostatic pressure resulting from the initial volume of 10 mL of fluid in the syringe, assuming a density of  $1000\text{kg/m}^3$ . The lowest stress is labelled  $\tau_1$  and corresponds to 1 mL in the syringe. The intermediate vertical dotted black lines labelled  $\tau_4$  and  $\tau_8$  correspond to a volume of 4 mL and 8 mL in the syringe, respectively

fluids classified as IDDSI level 3 pass also the fork drip test. Overall, the GTU suspensions show higher IDDSI levels than TU due to the higher viscosity of the continuum phase. The non-Newtonian TU solutions exhibit level 0 to level 3 IDDSI levels. Increasing the glycerol or thickener concentration leads to higher viscosity, consistency index, and to lower flow index. Accordingly, these fluids are classified as increasing IDDSI levels (Table 2), i.e. the residual volume left at 10 s increases. Therefore, the syringe flow test does not discriminate Newtonian and power-law fluids and assigns them to the same IDDSI level. For instance, the G9 and TU6 solutions are of level 3, but one is Newtonian, and the other exhibits a highly shear-thinning behaviour with  $n = 0.38$ . It is still unknown whether fluids with different rheological properties but with same IDDSI level behave similarly in vivo during swallowing.

The model follows very well the syringe flow dynamics for Newtonian and power-law fluids, as Fig. 3a and b show, except for the low glycerol concentrations, where a good prediction of the volume left at 10 seconds is obtained but a less satisfactory description of the whole dynamic than with the other concentrations. Looking at the entire dynamics (Fig. 3), the flow of fluids classified as levels 1, 2, and 3 is in excellent agreement with the theory throughout the tests. The results obtained with the GTU fluids show an excellent agreement too and are reported in Supplementary Fig. 8, for sake of brevity.

The theoretical predictions of the volume left at 10s, obtained without any fitting parameters, are in excellent agreement with the experimental measurements (Fig. 4). The theory only slightly overestimates the residues left by the TU2 at IDDSI level 0. However, this can be considered as

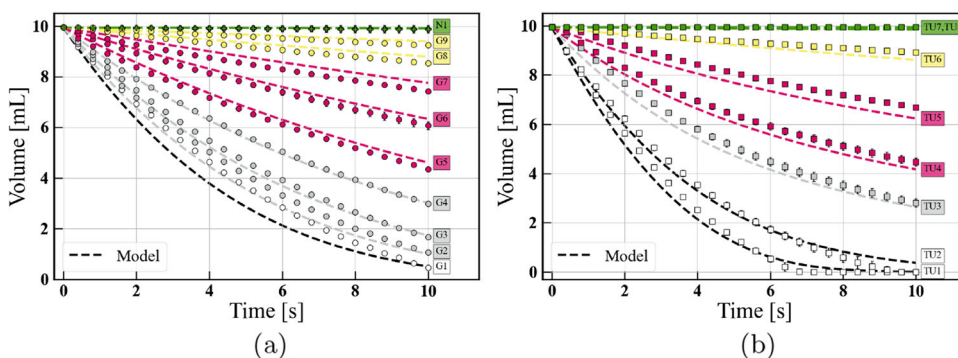


**Fig. 3** Evolution with time of the volume left in the syringe for **a** the different Newtonian fluids and **b** the different TU solutions considered. The marks show the experimental measurements, while the dashed lines show the theoretical predictions. The colours reflect the IDDSI levels.

The markers of level 0 liquids, leaving less than 1 mL in the syringe, are coloured in white, level 1 liquids in grey, level 2 in pink, level 3 in yellow

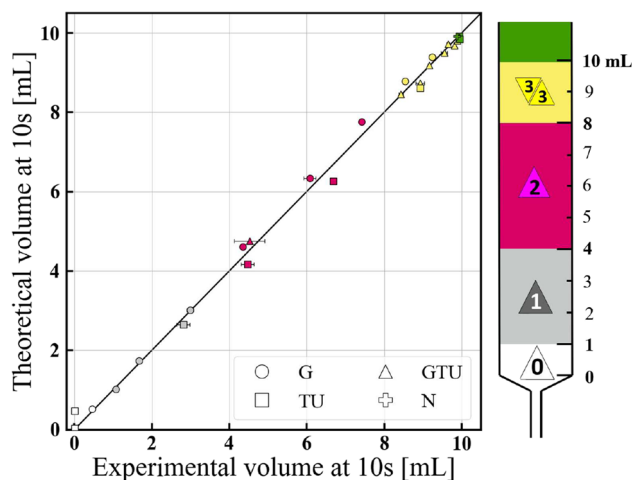


**Fig. 4** Volume left in the syringe at 10s: comparison of the theoretical predictions with the experimental measurements. The colours reflect the IDDSI levels. The markers of level 0 liquids, leaving less than 1 mL in the syringe, are coloured in white, level 1 liquids in grey, level 2 in pink, level 3 in yellow. The  $y = x$  straight line captures the data with  $R^2 = 0.997$ . NB: for some points, the error bars are smaller than the size of the markers

a minor limitation, since such low-viscosity beverages are not suitable for managing swallowing disorders. Such small overestimation may be linked to an overestimation of the surface tension effect in the model.

Overall, the experimental results and the theory are in good agreement. Thanks to the relative simplicity of the model (compared, for instance, to CFD simulations performed by Hanson et al. (2019)), it can be used to study the effect of fluid properties and geometrical parameters on the results of the IDDSI Syringe Flow Test systematically, as long as a power-law model can describe them and that they do not exhibit strong elastic properties (Mackley et al. 2013). Once validated against the experimental data for an extensive range of  $K$  and  $n$  values with the selection of G, TU, and GTU solutions and identified its limitations, our model can now be used to simulate the test outcomes for any virtual power-law fluids.

### Effect of the fluid rheology on the syringe test: a rheological map

The accuracy and low computational cost of the proposed model enabled the systematic simulation of the IDDSI syringe flow test for a wide range of rheological parameters  $K$  and  $n$ . The results of ten thousand simulations are condensed in the rheological map proposed in Fig. 5. Colours indicate the IDDSI levels predicted by the model for a given combination of  $K$  and  $n$ . At higher  $K$ , the fluids are thicker, while at lower  $n$ , they are more shear-thinning. The vertical dashed blue line, where  $n = 1$ ,

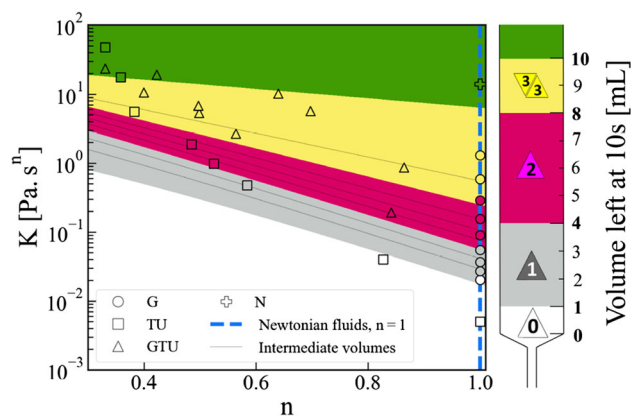


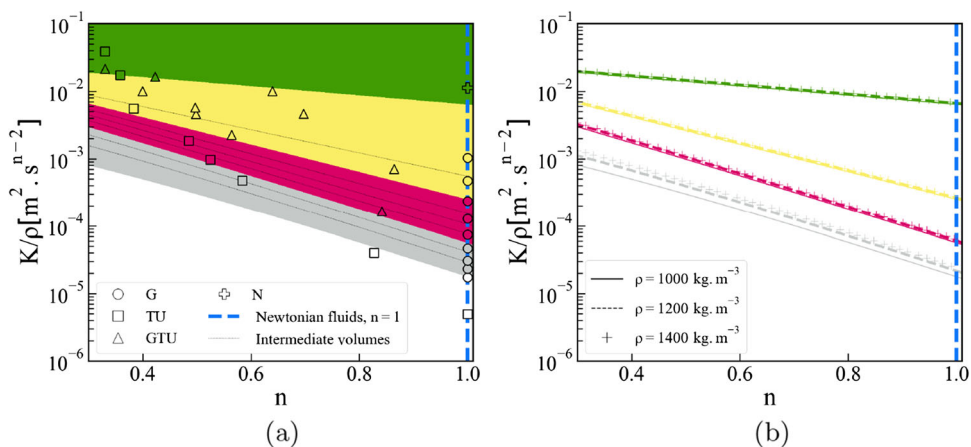
**Fig. 5** Rheological map describing the IDDSI levels for a range of the fluid rheological parameters  $K$  and  $n$ . The regions coloured according to the IDDSI levels are predicted theoretically considering  $\rho = 1000\text{kg}\cdot\text{m}^{-3}$ ,  $\sigma_{\text{water}} = 72\text{mN}\cdot\text{m}^{-1}$ , and  $R_{\text{min}} = 1\text{mm}$ . The vertical dotted line ( $n = 1$ ) represents the Newtonian fluids, and the dash-dotted lines are the intermediate volumes within each IDDSI levels. The experimental results are also coloured according to the experimental IDDSI level. The markers of level 0 liquids, leaving less than 1 mL in the syringe, are coloured in white, level 1 liquids in grey, level 2 in pink, level 3 in yellow. The shape of the mark depends on the type of fluid. The density of the Newtonian fluids used in the experiments differs from  $\rho = 1000\text{kg}\cdot\text{m}^{-3}$ , which explains some small differences between the level predicted by theory and experiments

represents Newtonian fluids. The map was obtained considering (i) water density  $\rho = 1000\text{kg}\cdot\text{m}^{-3}$ , (ii) water surface tension  $\sigma_{\text{water}} = 72\text{mN}\cdot\text{m}^{-1}$ , and (iii) an outlet radius of  $R_{\text{min}} = 1\text{mm}$ . As seen in “Rheological properties”, several suspensions of GTU and TU behave similarly as they are located close to each other on the map. GTU suspensions exhibit an intermediate behaviour, having higher flow index than TU suspensions. Experimental results are also presented with coloured symbols in Fig. 5, which confirms overall the excellent agreement already discussed in Fig. 4. However, among the Newtonian liquids, some level (colour) mismatch appear. These differences can be explained by the density of the glycerol solutions that is significantly higher than the density of  $1000\text{kg}\cdot\text{m}^{-3}$  considered in the simulations used to draw the rheological map. The effect of fluid density on the rheological map will be discussed later in the article.

This map represents visually the rheological borders between each IDDSI level and their dependency on  $K$  and  $n$ . Within each region, dotted boundaries are also drawn for intermediate residual volumes ( $2\text{mL}$ ,  $3\text{mL}$ ,  $5\text{mL}$ , etc.). These boundaries turn out to be rather straight. As shown by Wagner et al. (2017), a straight line in such diagram corresponds to a constant shear viscosity and shear rate. By fitting a straight line for each mean volume, i.e. respectively  $2.5\text{mL}$ ,  $6\text{mL}$ , and  $9\text{mL}$  for levels 1, 2, and 3, relevant mean shear rates were obtained for IDDSI levels 1, 2, and 3:  $213\text{ s}^{-1}$ ,  $330\text{ s}^{-1}$ ,  $53\text{ s}^{-1}$ . The mean shear rate depends therefore on the IDDSI level, which is a direct consequence of the imposed stress



**Fig. 6** **a** Rheological map presented in Fig. 5 re-scaled by the density  $\rho$ . The markers of level 0 liquids, leaving less than 1 mL in the syringe, are coloured in white, level 1 liquids in grey, level 2 in pink, level 3 in yellow. **b** The borders of the re-scaled rheological map are not significantly affected by a 20% or 40% increase in fluid density, confirming that the syringe flow test is governed by the kinematic viscosity



nature of the syringe test. Hence, the syringe test results cannot be related to the fluid viscosity at any specific shear rate, unlike it was proposed by Matsuyama et al. (2020).

As the IDDSI level increases, the borders become less dependent on the flow index  $n$  and more horizontal. Indeed, when a fluid is very viscous, the initial shear stress applied by the hydrostatic pressure induces only a very low average shear rate. Hence, the slope of the upper border of level 3 is low.

Another interesting piece of information is the relative areas occupied by each IDDSI level in the rheological map. The biggest regions are level 0 and the area above level 3, due to finite scale effects: on one side, the initial volume is fixed (10 mL); on the other side, the test duration is also fixed (10 s). Focusing on a single level, i.e. level 3, it can be noticed that a level 3 fluid can either be a thick Newtonian fluid like pure glycerol and a viscosity of approximately 1 Pa.s, or a much thicker TU suspension, with an order of magnitude higher viscosity at  $\dot{\gamma} = 1 \text{ s}^{-1}$ , but strongly shear-thinning. To the authors' knowledge, the equivalence of these extremely different rheological properties has never been investigated in vivo, and these results could become a source of inspiration for new clinical trials.

**Effect of the fluid density on the syringe test**

The results presented in the previous paragraph showed that the rheological properties have a strong impact on the test outcomes, but the rheological map and the borders between IDDSI levels are also influenced by the fluid density. Some Newtonian fluids with higher density appeared as outliers in Fig. 5, as shown by the colour mismatch with the theoretical regions obtained considering a fluid density  $\rho = 1000 \text{ kg.m}^{-3}$ . Figure 6a shows the rheological map of Fig. 5 re-scaled by dividing  $K$  by the density  $\rho$  and considering thus the kinematic viscosity, consistently with the gravity-driven nature of the test. This re-scaled rheological map captures

perfectly all experimental results and the effect of product densities.

To test further the robustness of this re-scaling, simulations were conducted increasing fluid density to  $\rho = 1200 \text{ kg.m}^{-3}$  and  $\rho = 1400 \text{ kg.m}^{-3}$ . The results are reported in Fig. 6b. A good superposition of the borders is observed for all densities and rheological parameters, suggesting that the IDDSI flow test is governed by the kinematic viscosity  $\nu = \eta/\rho$ , rather than the dynamic viscosity  $\eta$ . Small differences in the position of the boundary between level 0 and level 1 are probably due to the increasing effect of the Laplace counter-pressure for low-viscosity and low-density fluids. Understanding the important role that fluid density plays in the IDDSI flow test is particularly important, when using high density radio-opaque contrast agents to diagnose

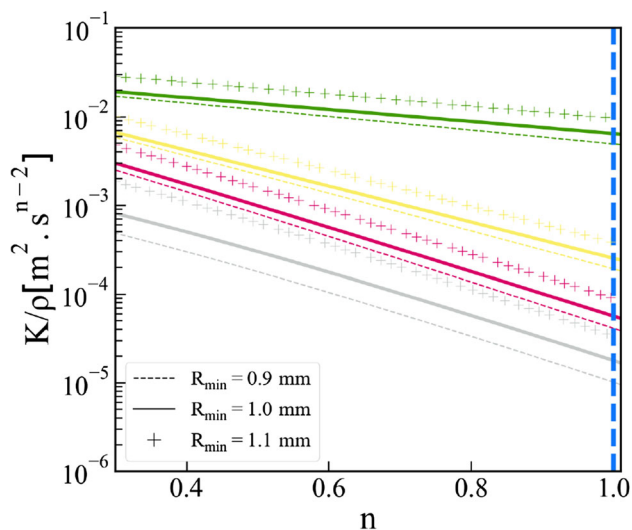


**Fig. 7** Effect of a 10% variation of the outlet radius on the borders (solid lines) of the rheological map presented in Fig. 5. The grey lines represent the boundary between level 0 and level 1, the pink between level 1 and level 2, yellow between level 2 and level 3, while the green ones represent the upper limits of level 3

swallowing disorders, since texture prescription should consider the effect of density changes.

### Effect of the nozzle radius on the syringe test

The sensitivity on the nozzle radius was also investigated, considering a 10% variation, i.e.  $R_{min} = 0.9\text{mm}$  and  $R_{min} = 1.1\text{mm}$ . As shown in Fig. 7, a larger radius leads to lower dissipation and faster flow, which raises the borders of the levels in the rheological map. A wider radius reduces also the Laplace counterpressure, further accelerating the flow. The effect of nozzle radius on viscous dissipation is very strong (4th power for Newtonian fluids), and this dimension should be controlled precisely across syringes to guarantee a consistent IDDSI classification.

### Conclusion

This study sheds new light on the effect of fluid properties on the gravity-driven flow in a vertical syringe, widely used for the IDDSI classification of texture-modified beverages to manage swallowing disorders.

Experimental observations confirm that the syringe test does not discriminate between Newtonian and non-Newtonian fluids and that several fluids with different rheological properties are classified in the same way. Fluid density has also an important effect of the classification. The theory developed in this study offers excellent predictions of the remaining volumes in the syringe after 10 s, for a wide range of power-law fluids and describes well the dynamics, confirming the relevance of the different assumptions made.

The theory was used to propose an original rheological map linking the IDDSI levels to the rheological properties and the density of the fluid. The flow and the test outcome are sensitive to the fluid density and to nozzle geometry, particularly for low viscosity fluids. It is also demonstrated that different IDDSI levels are effectively flowing at different average shear rates in the nozzle. This suggests that the common attempt to relate the syringe flow and the viscosity at  $50\text{s}^{-1}$  lacks of relevance.

An important impact of the results presented in this study is to increase awareness that the IDDSI flow test is driven by the kinematic, rather than the dynamic viscosity. Fluids with very similar dynamic viscosity but significantly different densities may be classified differently. This study will also hopefully inspire new clinical trials to confirm that Newtonian and non-Newtonian fluids classified similarly in the IDDSI flow test do indeed flow similarly during human swallowing. According to the authors' knowledge, such clinical evidence is not yet available. Should clinical results suggest that the syringe test needs to be improved, the theory developed in this study could be used to devise improved

testing procedures. Interesting directions for future research comprise the extension of this study to viscoplastic and viscoelastic fluids.

**Supplementary Information** The online version contains supplementary material available at <https://doi.org/10.1007/s00397-024-01449-9>.

### Declarations

**Conflict of interest** The authors declare no competing interests.

### References

- Clavé P, Shaker R (2015) Dysphagia: current reality and scope of the problem. *Nat Rev Gastroenterol Hepatol* 12(5):259–270. <https://doi.org/10.1038/nrgastro.2015.49>
- Cote C, Giroux A, Villeneuve-Rheaume A, Gagnon C, Germain I (2020) Is IDDSI an evidence-based framework? A relevant question for the frail older population. *Geriatrics* 5(4). <https://doi.org/10.3390/geriatrics5040082>
- Digilov RM (2008) Capillary rise of a non-Newtonian power law liquid: impact of the fluid rheology and dynamic contact angle. *Langmuir* 24(23):13663–13667. <https://doi.org/10.1021/la801807j>. Publisher: American Chemical Society
- Hanson B, Jamshidi R, Redfearn A, Begley R, Steele CM (2019) Experimental and computational investigation of the IDDSI flow test of liquids used in dysphagia management. *Ann Biomed Eng* 47(11):2296–2307. <https://doi.org/10.1007/s10439-019-02308-y>
- Hanson B, Jamshidi R, Redfearn A, Begley R, Steele CM (2019) Experimental and computational investigation of the IDDSI flow test of liquids used in dysphagia management. *Ann Biomed Eng* 47(11):2296–2307. <https://doi.org/10.1007/s10439-019-02308-y>
- IDDSI: BD syringes for IDDSI flow test. <https://iddsi.org/IDDSI/media/images/FrameworkDocuments/BD-Syringes-for-IDDSI-Flow-Test-International-Codes.pdf>. Accessed: 21-12-18
- Mackley MR, Tock C, Anthony R, Butler SA, Chapman G, Vadillo DC (2013) The rheology and processing behavior of starch and gum-based dysphagia thickeners. *J Rheol* 57(6):1533–1553. <https://doi.org/10.1122/1.4820494>. Publisher: The Society of Rheology
- Matsuyama S, Nakauma M, Funami T, Yamagata Y, Kayashita J (2020) The influence of syringe geometry on the International Dysphagia Diet Standardisation Initiative flow test. *Int J Food Sci Technol* 55(8):2962–2969. <https://doi.org/10.1111/ijfs.14559>
- Matsuyama S, Nakauma M, Funami T, Yamagata Y, Kayashita J (2020) The influence of syringe geometry on the International Dysphagia Diet Standardisation Initiative flow test. *Int J Food Sci Technol* 55(8):2962–2969. <https://doi.org/10.1111/ijfs.14559>
- Roussel N, Le Roy R (2005) The Marsh cone: a test or a rheological apparatus? *Cem Concr Res* 35(5):823–830. <https://doi.org/10.1016/j.cemconres.2004.08.019>
- Roussel N, Le Roy R (2005) The Marsh cone: a test or a rheological apparatus?. *Cement and Concrete Research* 35(5):823–830. <https://doi.org/10.1016/j.cemconres.2004.08.019>
- Schindelin J, Arganda-Carreras I, Frise E, Kaynig V, Longair M, Pietzsch T, Preibisch S, Rueden C, Saalfeld S, Schmid B, Tinevez J-Y, White DJ, Hartenstein V, Eliceiri K, Tomancak P, Cardona A (2012) Fiji: an open-source platform for biological-image analysis. *Nat Methods* 9(7):676–682. <https://doi.org/10.1038/nmeth.2019>. Number: 7 Publisher: Nature Publishing Group

Steele CM, Alsanei WA, Ayanikalath S, Barbon CEA, Chen J, Cichero JAY, Coutts K, Dantas RO, Duivesteyn J, Giosa L, Hanson B, Lam P, Lecko C, Leigh C, Nagy A, Namasivayam AM, Nascimento WV, Odendaal I, Smith CH, Wang H (2015) The influence of food texture and liquid consistency modification on swallowing physiology and function: a systematic review. *Dysphagia* 30(1):2–26. <https://doi.org/10.1007/s00455-014-9578-x>. Company: Springer Distributor: Springer Institution: Springer Label: Springer Number: 1 Publisher: Springer, US

Sutera SP, Skalak R (1993) The history of Poiseuille's law. *Annu Rev Fluid Mech* 25(1):1–20. <https://doi.org/10.1146/annurev.fl.25.010193.000245>

Wagner CE, Barbati AC, Engmann J, Burbidge AS, McKinley GH (2017) Quantifying the consistency and rheology of liquid foods using fractional calculus. *Food Hydrocolloids* 69:242–254. <https://doi.org/10.1016/j.foodhyd.2017.01.036>

**Publisher's Note** Springer Nature remains neutral with regard to jurisdictional claims in published maps and institutional affiliations.

Springer Nature or its licensor (e.g. a society or other partner) holds exclusive rights to this article under a publishing agreement with the author(s) or other rightsholder(s); author self-archiving of the accepted manuscript version of this article is solely governed by the terms of such publishing agreement and applicable law.